

Selective hydrogenation improves interface properties of high-*k* dielectrics on 2D semiconductors

Yulin Yang^{1, #}, Tong Yang^{2, #}, Tingting Song³, Jun Zhou⁴, Jianwei Chai⁴, Lai Mun Wong⁴, Hongyi Zhang¹, Wenzhang Zhu¹, Shijie Wang^{4, *}, and Ming Yang^{2, *}

¹ Fujian Provincial Key Laboratory of Optoelectronic Technology and Devices, School of Optoelectronic and Communication Engineering, Xiamen University of Technology, Xiamen, 361024, China

² Department of Applied Physics, The Hong Kong Polytechnic University, Hung Hom, Kowloon, Hong Kong SAR, China

³ College of Physics and Space Science, China West Normal University, Nanchong, 637002, China

⁴ Institute of Materials Research and Engineering, Agency for Science, Technology and Research (A*STAR), 2 Fusionopolis Way, Innovis, 138634, Singapore

These authors contributed equally to this work.

* Author to whom correspondence should be addressed:

M.Y. (mingyang@polyu.edu.hk) or S.J.W. (sj-wang@imre.a-star.edu.sg)

ABSTRACT:

The integration of high- k dielectrics with two-dimensional (2D) semiconductors is a critical step towards high-performance nanoelectronics, which however remains challenging due to high density of interface states and the damage to the monolayer 2D semiconductors. In this study, we propose a selective hydrogenation strategy to improve the interface properties while do not affect the 2D semiconductors. Using the interface of monolayer MoS₂ and silicon nitride as an example, we show substantially improved interface properties for electronic applications after the interfacial hydrogenation, as evidenced by reduced inhomogeneous charge redistribution, increased band offset, and untouched electronic properties of MoS₂. Interestingly, this hydrogenation process selectively occurs only at the silicon nitride surface and is compatible with the current semiconductor fabrication process. We further show that this strategy is general and applicable to other interfaces between high- k dielectrics and 2D semiconductors such as HfO₂ on the monolayer MoS₂. Our results demonstrate a *simple yet viable* way to improve the interfacial properties for integrating many high- k dielectrics on a broad range of two-dimensional transition metal disulfide semiconductors.

KEY WORDS:

Two-dimensional materials, high- k dielectrics, molybdenum disulfide, interfacial properties, transition metal disulfide

INTRODUCTION

Two-dimensional (2D) semiconducting materials are appealing for nanoelectronic applications in the post-Moore era as their ultra-thin thickness can help minimize the short channel effect confronted with current Si based technologies.^{1, 2} Among them, monolayer transition metal disulfides (TMDs) such as MoS₂ and WS₂ have attracted tremendous interest as promising channel materials for electronic or optoelectronic devices due to their stability, direct band gaps, tunable electronic and optical properties, and many other excellent physical properties.³⁻¹⁰ The monolayer MoS₂ based nanotransistors have shown encouraging device performance such as a high on/off ratio.¹¹⁻¹³ However, to utilize monolayer TMDs in practical electronic applications, there remain many challenges¹⁴, which include the large-scale growth of high-quality TMDs layers¹⁵⁻¹⁹, metal contact with low resistance²⁰⁻²⁵, and the integration of high-*k* dielectrics.²⁶⁻²⁹

In particular, for electronic applications, the integration of high-*k* dielectrics is highly desired as their large dielectric constants can effectively screen the scattering from charge impurities and thus improve the device's performance.^{30, 31} However, it is found difficult to achieve high-quality interfaces between high-*k* dielectrics and monolayer TMDs which results in high interface state density.^{28, 29} Currently, a high-quality interface can be realized by van der Waals (vdW) integration of *h*-BN or CaF₂ layers on TMDs semiconductors³²⁻³⁴, but the sophisticated integration process and the difficulty in direct growth of high-quality vdW layers impede its large-scale practical applications. While various attempts have been made to directly deposit high-*k* oxides such as HfO₂³⁵, Al₂O₃^{36, 37} and ZrO₂³⁸ on TMDs layers using atomic layer deposition (ALD) or sputtering technique, their interfacial properties are still much inferior to that of HfO₂/Si and need further improvement.^{29, 39}

One such endeavor is interface engineering, which includes interface passivation by annealing^{40, 41}, and utilizing interface seeding or buffer layers^{28, 29, 42}. These strategies have brought some improvement from their respective effects but may also raise new problems such as the damage of the 2D TMDs semiconductors and accordingly deteriorated electronic properties.^{28, 29} Thus, it is highly desirable to develop a holistic strategy that can effectively passivate the interfacial dangling bonds of high-*k* dielectrics but does not deteriorate the 2D semiconductors. In this study, we propose selective hydrogenation as such an ideal strategy, thanks to the fact that the hydrogen atoms are prone to be adsorbed on the surface of high-*k* dielectrics but inert to the basal planes of 2D TMDs. We use the interface between monolayer MoS₂ and β -Si₃N₄ (0001) as an example to deliver the concept and apply this strategy to another interface between MoS₂ and HfO₂ to demonstrate its generality.

METHOD

All the calculations were performed using density-functional theory (DFT) based the Vienna Ab initio Simulation Package (VASP.5.4.4.18) with the Perdew-Burke-Ernzerhof (PBE) functional and the projector-augmented wave (PAW) potentials.⁴³⁻⁴⁵ The cutoff energy for the plane wave expansion was set to 500 eV. Γ -centered 9×9×4, 12×12×1, 6×6×1, and 9×9×1 *k*-point meshes were used to sample the first Brillouin zone of bulk β -Si₃N₄, monolayer MoS₂, and the interface of monolayer MoS₂ on β -Si₃N₄ (0001) and *c*-HfO₂ (111), respectively. A vacuum layer with a thickness of 15 Å was used for all slab structures to minimize the artificial Coulomb interaction between two adjacent surfaces. For the interface structures, the vdW correction has been included by Grimme's DFT-D3 method.⁴⁶ For all calculations, the electronic and ionic convergence criteria were set to 10⁻⁵ eV and 0.01 eV/Å, respectively. The calculated lattice constants of β -Si₃N₄ and MoS₂ monolayer are

a=b=7.659 Å and c=2.925 Å, and 3.184 Å, and the corresponding PBE band gaps are 4.24 eV and 1.66 eV, respectively. All these results are well consistent with previous studies.⁴⁷⁻⁵¹

The interface structures were constructed by placing the (4×4×1) monolayer MoS₂ supercell on the ($\sqrt{3} \times \sqrt{3} \times 1$) β -Si₃N₄ (0001) surface without/with surface hydrogen passivation, in which a 3.97% compressive strain was applied to the Si₃N₄. This strain yields a reduced PBE band gap by ~0.2 eV in the Si₃N₄ (see Fig. S1 in the Supporting Information), while the main electronic structure does not change much compared with that of the pristine bulk Si₃N₄. The thickness of the β -Si₃N₄ (0001) surface was set to 7 atomic layers, the bottom layer of which was passivated using hydrogen atoms. In the interface structures, dipole correction was applied.⁵² To examine interfacial stability of monolayer MoS₂/hydrogen passivated β -Si₃N₄ (0001), *ab initio* molecular dynamics simulations were performed on the interface supercell, where the canonical ensemble (NVT) and the Nosé heat bath were adopted with a time step of 1 fs and a time length of 6 ps

The interfacial interaction strength between monolayer MoS₂ and dielectrics (D, Si₃N₄ or HfO₂) can be estimated from the adsorption energy (E_{ad}) as defined below:

$$E_{ad} = E_{\text{MoS}_2+D} - E_{\text{MoS}_2} - E_D, \quad (1)$$

where E_{MoS_2+D} is the total energy of the hybrid interface structure for MoS₂ on the dielectrics, and E_{MoS_2} and E_D are the total energy of the isolated MoS₂ monolayer and the dielectric (Si₃N₄ or HfO₂) surface, respectively. Similarly, the charge redistribution $\Delta\rho$ for MoS₂ monolayer on the dielectric surface is defined as:

$$\Delta\rho = \rho_{\text{MoS}_2+D} - \rho_{\text{MoS}_2} - \rho_D, \quad (2)$$

in which ρ_{MoS_2+D} is the charge density of the hybrid interface structure for MoS₂ on the dielectric, and ρ_{MoS_2} and ρ_D are the charge density of the isolated MoS₂ monolayer and the dielectric (Si₃N₄ or HfO₂) surface, respectively.

RESULTS AND DISCUSSIONS

Silicon nitride (Si₃N₄) has a large band gap and high thermal stability, which has been widely applied in current Si based electronic devices.^{49, 50, 53} It was reported that high-quality Si₃N₄ thin films can be deposited on graphene^{48, 54, 55}, while the electronic properties of the latter does not change much.⁵⁴ Furthermore, Si₃N₄ might be a better choice than the metal oxides as a high-*k* dielectric because it does not contain metallic ions which tend to interact strongly with 2D TMDs.^{47, 56, 57} Thus, in this study, we use the interface between monolayer MoS₂ and β -Si₃N₄ as a model example to study the hydrogenation effect on the interface properties.

We have constructed various interface structures by sliding the MoS₂ on the Si₃N₄ surface. The energy difference among these configurations is within 12 meV (see Fig. S2(a)), inferring a weak interfacial interaction. The top and side view of the most stable interface configuration is shown in Fig. S2(b) and Fig 1(a), respectively, in which the interfacial S atoms of MoS₂ tend to arrange near the interfacial Si atoms of Si₃N₄ to maximize the potential bonding. Similar trend has been reported at the interfaces of MoS₂/HfO₂ or high-*k* dielectrics/graphene.^{47, 58, 59} The interface spacing between monolayer MoS₂ and β -Si₃N₄ (0001) is about 2.9 Å, at the lower bound of the vdW interaction range, further indicating weak interface interaction. The interface interaction strength can also be measured from the adsorption energy (-23.2 meV/Å²). This value is slightly higher than that of bi-layer MoS₂ (-22.4 meV/Å²), but it is much

smaller than those of other high-k dielectric/TMDs interfaces such as MoS₂/HfO₂ and MoS₂/SiO₂.^{47, 57, 60}

The projected density of states (PDOSs) of monolayer MoS₂ on β -Si₃N₄ (0001) is shown in Figs. 1(c-e). One important observation is that the electronic structure of monolayer MoS₂ is nearly intact in the presence of the Si₃N₄ due to relatively weak interaction between them. As the PDOS shown in Fig. 1(c), the monolayer MoS₂ remains semiconducting with a PBE gap of ~1.6 eV. This is highly desired because a sizable band gap in semiconductors enables a stable device operation with a large on/off ratio. However, due to the dangling bonds in β -Si₃N₄ (0001) (see Fig. S3) induced mid-gap states, orbital hybridization is seen between MoS₂ and Si₃N₄. As Figs. 1(b-d) show, the Mo e_g orbitals couple with the p orbitals of Si and N ions near the valence band edge, while at the conduction edge, the hybridization among Mo e_g, S p_z orbital and Si p_z orbital is more noticeable. This orbital hybridization leads to insignificant band offsets between MoS₂ and Si₃N₄, which is unfavorable for device applications. To minimize the tunneling current in semiconductor devices, the valence and conduction band offset between the semiconductor (e.g., MoS₂ in this study) and the gate dielectric (e.g., Si₃N₄ here) should be larger than 1 eV.³⁰ In addition, the interfacial interaction causes charge redistribution at the interface (see Fig. 1(a)), where the accumulated charges are closer to Si₃N₄ surface while the depleted charges are more pronounced near MoS₂ side. The charge redistribution induces electron-hole puddles in monolayer MoS₂, as shown in Fig. 1(b). This is another detrimental effect for electronic device applications as the electron-hole puddles can be charge scattering centers which reduce the carrier mobility.⁶¹

Since the degraded interface properties are mainly due to the dangling bonds at the β -Si₃N₄ (0001) surface, one natural attempt for improving the interface

properties is to passivate them. We note that the hydrogenation process has been widely used in semiconductor technologies to passivate the intrinsic defects.⁶² Such process may also be applied to passivate the dangling bonds of the β -Si₃N₄ (0001) surface considered in this study. After passivation (see the atomic structures in Fig. S4(a)), the dangling bonds induced states nearly vanish as confirmed by the PDOSs in Fig. S4(b). Consequently, the interfacial interaction between monolayer MoS₂ and hydrogen passivated β -Si₃N₄ (0001) surface is further weakened. The calculated adsorption energy (see Fig. 2(a)) decreases slightly to -18.2 meV/Å². The charge redistribution is shown in Fig. 2(b) and (c), which clearly suggests that the weaker interfacial interaction results in much less pronounced interfacial charge redistribution, as well as the suppressed electro-hole puddles on the Mo atomic plane.

After the hydrogen passivation on the β -Si₃N₄ (0001) surface, the orbitals near Fermi level between monolayer MoS₂ and Si₃N₄ are well separated. From Fig. 2(d), we can see that the valence band edge now is contributed by p orbital from Si₃N₄, while the states contributed by Mo d orbital are located at -0.98 eV below the Fermi level. In contrast, the conduction band edge is mainly derived from Mo d orbital, and the contribution from p orbital of Si₃N₄ starts from ~4.88 eV and above. This leads to a type-II band offset between monolayer MoS₂ and Si₃N₄, in which the valence band (VBO) and conduction band offset (CBO) can be estimated to be 0.98 and 3.3 eV at the PBE level, respectively. It should be noted that these band offset values might be underestimated, which could be larger if the quasiparticle corrections or hybrid functionals are used. With the hydrogen passivation, we also find improvement on the electronic properties of monolayer MoS₂. As shown in Fig. 2(e), the electronic structure of monolayer MoS₂ on the hydrogen passivated Si₃N₄ is nearly identical to that of free-standing monolayer MoS₂. Thus, we can see that using this simple hydrogenation

process, the interface properties of MoS₂/Si₃N₄ are improved remarkably as evidenced by the large band offsets, suppressed electron-hole puddles, and intact electronic properties of MoS₂.

More importantly, the hydrogenation process is energetically selective to β -Si₃N₄ (0001) surface. As shown in Fig. 3(a) shows, the adsorption energy for hydrogen atom on top of Si site at the Si₃N₄ surface is -0.23 eV, and the lowest adsorption energy on the top of the N sites is -1.11 eV due to the dangling bonds of N ions at the surface. The negative adsorption energy indicates that the hydrogen adsorption is energetically favorable, and the hydrogenation can occur spontaneously even at low temperature. In contrast, the energy for hydrogen atoms adsorbed on the monolayer MoS₂ is calculated to be 1.84 eV, consistent with previous studies.⁶³ The large positive adsorption energy suggests that the hydrogenation on the monolayer MoS₂ is energetically unfavorable, which is less likely to happen even at a high processing temperature. Further quantum mechanical molecular dynamics simulation shows that the hydrogen passivated MoS₂/Si₃N₄ interface is thermodynamically stable at the high temperature of 800 K. From Fig. 3(b) and Fig. S(5), it is noted that the variation of interfacial Si-H and N-H bond length is within 0.2 Å during the MD simulation, suggesting that the Si₃N₄ surface adsorbs hydrogen atoms so strongly that they are unlikely to diffuse to monolayer MoS₂ even at a temperature of 800 K (see Fig. 3(c)). This implies that the spontaneously selective hydrogenation process is compatible and stable with current semiconductor device fabrication processes, as most of them are conducted below 800 K.⁶⁴

Next, we show that the hydrogenation process is applicable for improving interface properties of other high-*k* oxides and monolayer MoS₂. Since HfO₂ has been widely used in current electronic devices, we use it as a model example to further

examine the hydrogenation effect. It has been reported that Hf-terminated HfO₂ interacts strongly with MoS₂, leading to inferior electronic properties, while the interface between O-terminated HfO₂ and MoS₂ shows improved interface performance.⁴⁷ Thus, we focus on the interface of Hf-terminated HfO₂ and monolayer MoS₂ without/with the interfacial hydrogenation. As Figs. 4(a) and (c) show, at the interface of Hf-terminated HfO₂ and monolayer MoS₂, it forms interfacial covalent Hf-S bonds. This induces noticeable charge transfer from HfO₂ into MoS₂, making the MoS₂ metallic. Similarly, the interface properties can be improved using the hydrogenation process. Figures 4(b) and (d) are the charge redistribution and local density of states (LDOS) for monolayer MoS₂ on the hydrogen passivated Hf-HfO₂ (0001) surface, respectively. The reduced interfacial charge redistribution and the suppressed mid-gap metallic states in MoS₂ clearly suggest that better interface properties are reached by the selective hydrogen passivation.

It has been noted that 2D materials with HfO₂ thin films grown by atomic layer deposition (ALD) technique show better device performance than those using sputtering or physical vapor deposition (PVD).⁶⁵ We argue that the underlying mechanisms, in addition to the film uniformity and quality, could be partially ascribed to unintended hydrogen passivation on the high-*k* oxide film. In ALD process, the Hf metal-based precursor and water vapor are used for the deposition of HfO₂⁶⁶, in which residual hydrogen source might evolve to passivate the dangling bonds, whereas the high vacuum required in sputtering or PVD process leads to negligible residual hydrogen sources. Thus, we believe that the interface between high-*k* dielectrics and MoS₂ can be further improved by intentionally depositing the high-*k* dielectric films in the hydrogen environment at the first few cycles. Please note that the effectiveness of this interfacial hydrogenation strategy is strongly dependent on the difference in the

hydrogen adsorption on 2D materials and high- k dielectrics. If hydrogen interacts strongly on the 2D materials such as graphene⁶⁷ or phosphorene⁶⁸, the hydrogenation process would result in undesired hydrogen adsorption on the 2D materials as it will change the electronic properties of 2D materials. On the contrary, as long as a 2D material is unfavorable to bind hydrogen, the hydrogenation process proposed here is beneficial to its integration with high- k dielectrics. The beneficial effects of this hydrogenation strategy on the interface integration are two-fold: one is to passivate the dangling bonds in the high- k dielectrics, resulting in reduced interface state density; the other is to passivate the native defects in 2D TMDs, which can further improve electronic properties of the 2D semiconductors.

In conclusion, we report a simple yet effective strategy to improve the interfacial properties of high- k dielectrics and 2D semiconductors, as supported by the substantially improved electronic properties at the interface between Si_3N_4 and monolayer MoS_2 using the proposed selective hydrogenation process. This hydrogenation process spontaneously occurs on Si_3N_4 , leaving the monolayer MoS_2 nearly intact. We reveal that the hydrogenated $\text{MoS}_2/\text{Si}_3\text{N}_4$ interface is stable at high temperatures, which is compatible with the current semiconductor fabrication process. We further show that the interfacial hydrogenation strategy can be applied for the integration of other high- k dielectrics on MoS_2 monolayer. Given similar surface chemistry among TMD semiconductors, this hydrogenation process can be extended to the interfaces of many high- k dielectrics and a broad range of TMDs such as MoS_2 , WS_2 , or HfS_2 , as well as some transition metal dichalcogenides such as MoSe_2 or WSe_2 , or other 2D materials that are inert to hydrogen adsorption, enabling us to boost the development of 2D semiconductors based nanoelectronic devices.

Acknowledgements

M.Y. acknowledges the funding support (project IDs: 1-BE47 and ZE2F) from The Hong Kong Polytechnic University. We acknowledge Centre for Advanced 2D Materials and Graphene Research at National University of Singapore, and the National Supercomputing Centre of Singapore for providing computing resources.

Conflict of Interest

The authors declare no conflict of interest.

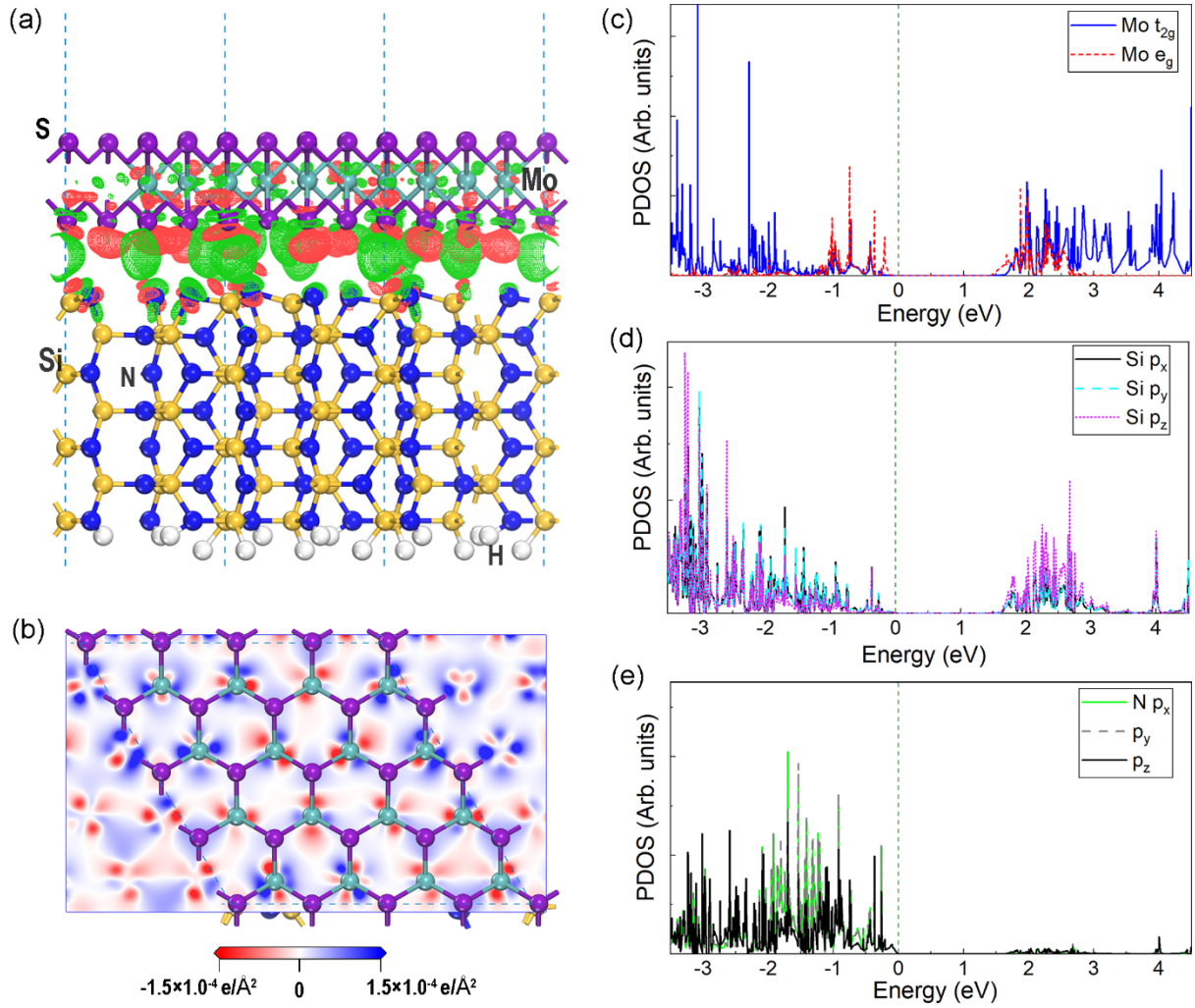


Figure 1. Interface properties between monolayer MoS₂ and β -Si₃N₄ (0001). (a) top and (b) side view of the most stable configuration for monolayer MoS₂ on β -Si₃N₄ (0001), in which the red and green dots in (a) denote the depleted and accumulated charge density visualized by an iso-surface value of $1.5 \times 10^{-4} \text{ e}/\text{\AA}^3$, respectively. The red and blue colour in (b) denotes charge puddles on the Mo plane. The projected density of states (PDOSs) for Mo (c), Si (d) and N (e), where the Fermi level is set to 0 eV.

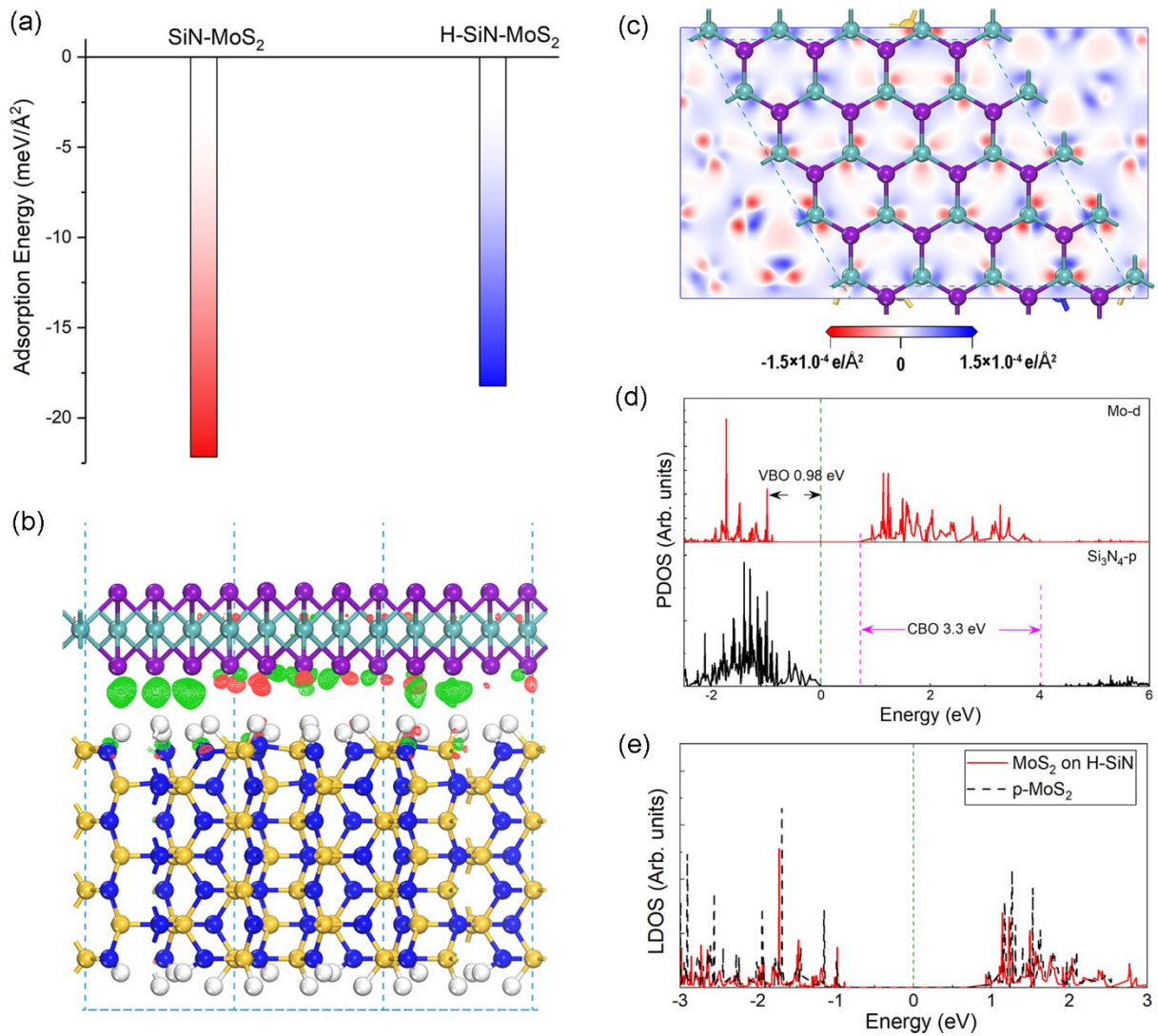


Figure 2. Interface properties of monolayer MoS₂ on hydrogenated β -Si₃N₄ (0001). (a) Adsorption energy of monolayer MoS₂ on β -Si₃N₄ (0001) w/o surface hydrogenation. (b) The side view of interface structure for monolayer MoS₂ on hydrogenated β -Si₃N₄ (0001) superimposed with visualized charge density redistribution using an iso-surface value of $1.5 \times 10^{-4} e/\text{\AA}^3$, in which red and green dots denote the depleted and accumulated charge density, respectively. (c) The charge puddles distributed on the Mo plane. (d) The PDOSs on Mo d orbital and p orbitals of central Si₃N₄ layer. (e) LDOSs of MoS₂ monolayer on hydrogenated β -Si₃N₄ (0001) and the pristine monolayer MoS₂.

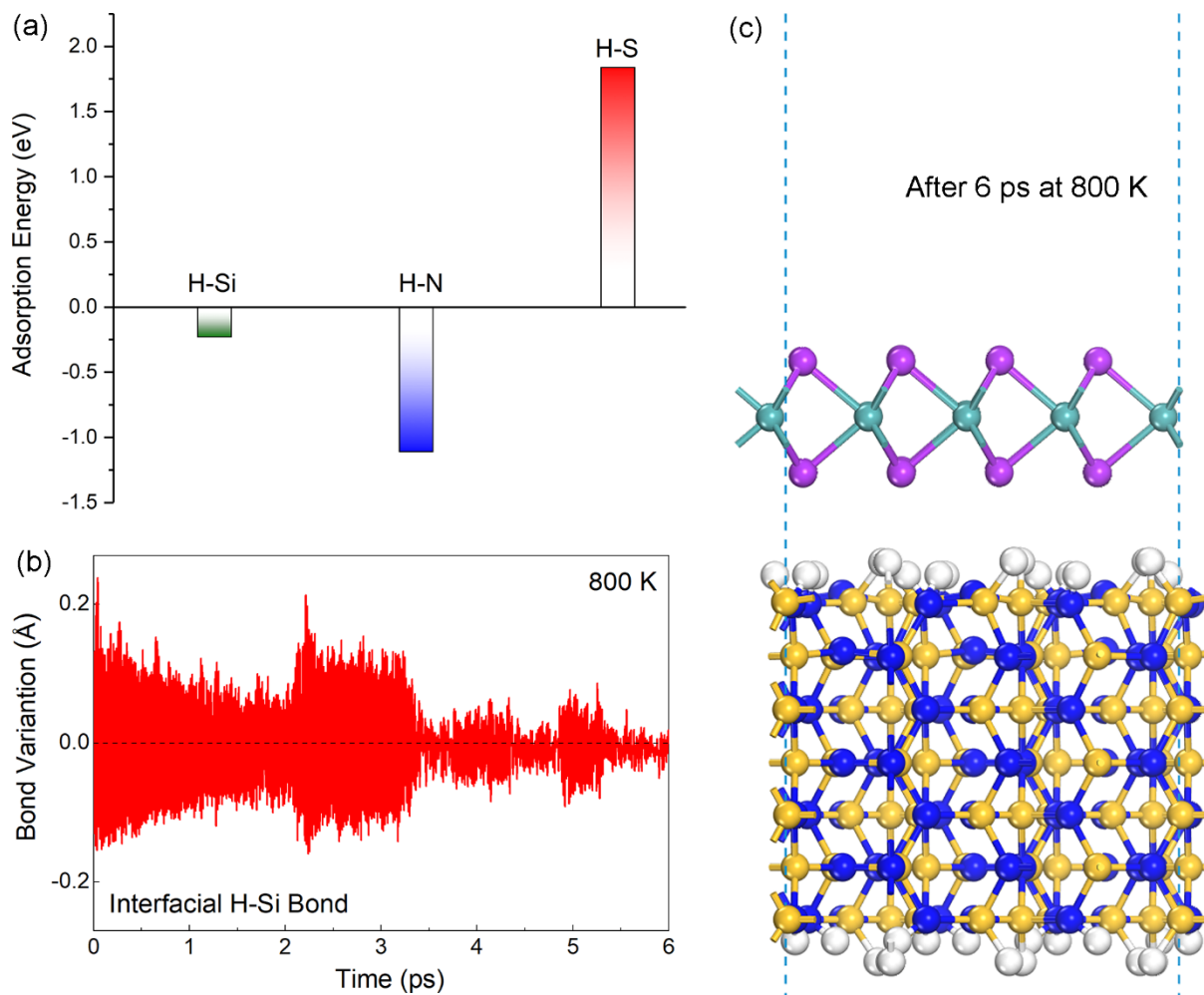


Figure 3. Hydrogenation selectivity and stability. (a) The hydrogen adsorption energy on β -Si₃N₄ (0001) and monolayer MoS₂. (b) The interface Si-H bond variation during the molecular dynamic (MD) simulation at the temperature of 800 K. (c) The final atomic structure (side view) of MoS₂ monolayer on the hydrogenated β -Si₃N₄ (0001) surface after the 6 ps MD simulation.

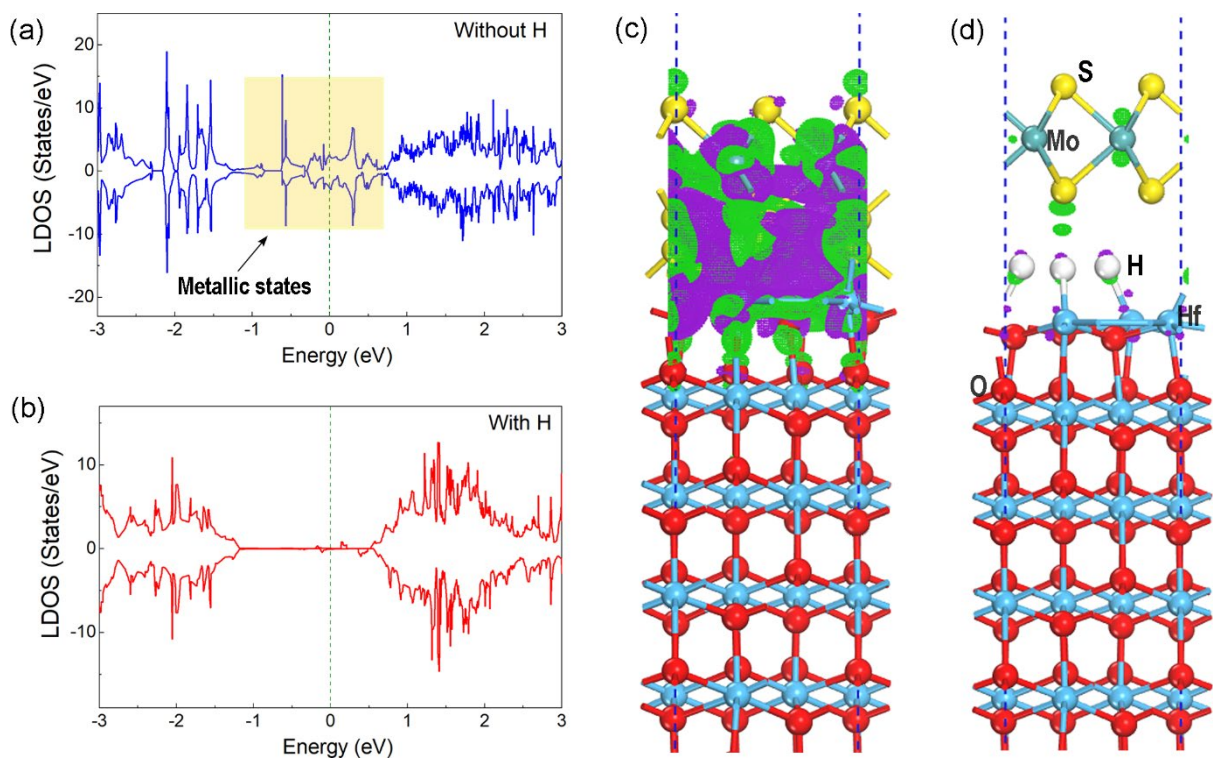


Figure 4. Hydrogenation effect on interface properties of monolayer MoS₂ on Hf-terminated HfO₂ (0001) surface. The LDOSs of MoS₂ monolayer on (a) HfO₂ (0001) surface and (b) hydrogen passivated HfO₂ (0001) surface. The charge density redistribution for MoS₂ monolayer on (ac) HfO₂ (0001) surface and (d) hydrogen passivated HfO₂ (0001) surface, where the green and purple dots denote the excess and accumulated charge density visualized by an iso-surface value of $3.0 \times 10^{-3} \text{ e}/\text{\AA}^3$, respectively.

References

1. G. Fiori, F. Bonaccorso, G. Iannaccone, T. Palacios, D. Neumaier, A. Seabaugh, S. K. Banerjee and L. Colombo, *Nature Nanotechnology*, 2014, **9**, 768-779.
2. M.-Y. Li, S.-K. Su, H.-S. P. Wong and L.-J. Li, 2019, **567**, 169-170.
3. K. F. Mak, C. Lee, J. Hone, J. Shan and T. F. Heinz, *Physical Review Letters*, 2010, **105**, 136805.
4. S. Z. Butler, S. M. Hollen, L. Cao, Y. Cui, J. A. Gupta, H. R. Gutiérrez, T. F. Heinz, S. S. Hong, J. Huang and A. F. Ismach, *ACS Nano*, 2013, **7**, 2898-2926.
5. Y. Yoon, K. Ganapathi and S. Salahuddin, *Nano Letters*, 2011, **11**, 3768-3773.
6. G. Wang, A. Chernikov, M. M. Glazov, T. F. Heinz, X. Marie, T. Amand and B. Urbaszek, *Reviews of Modern Physics*, 2018, **90**, 021001.
7. G.-B. Liu, D. Xiao, Y. Yao, X. Xu and W. Yao, *Chemical Society Reviews*, 2015, **44**, 2643-2663.
8. Q. H. Wang, K. Kalantar-Zadeh, A. Kis, J. N. Coleman and M. S. Strano, *Nature Nanotechnology*, 2012, **7**, 699-712.
9. K. S. Novoselov, D. Jiang, F. Schedin, T. Booth, V. Khotkevich, S. Morozov and A. K. Geim, *Proceedings of the National Academy of Sciences*, 2005, **102**, 10451-10453.
10. V. K. Sangwan, H.-S. Lee, H. Bergeron, I. Balla, M. E. Beck, K.-S. Chen and M. C. Hersam, *Nature*, 2018, **554**, 500-504.
11. B. Radisavljevic, A. Radenovic, J. Brivio, V. Giacometti and A. Kis, *Nature Nanotechnology*, 2011, **6**, 147-150.
12. S. Kim, A. Konar, W.-S. Hwang, J. H. Lee, J. Lee, J. Yang, C. Jung, H. Kim, J.-B. Yoo and J.-Y. Choi, *Nature Communications*, 2012, **3**, 1-7.
13. S. B. Desai, S. R. Madhvapathy, A. B. Sachid, J. P. Llinas, Q. Wang, G. H. Ahn, G. Pitner, M. J. Kim, J. Bokor and C. Hu, *Science*, 2016, **354**, 99-102.
14. N. Briggs, S. Subramanian, Z. Lin, X. Li, X. Zhang, K. Zhang, K. Xiao, D. Geohegan, R. Wallace and L.-Q. Chen, *2D Materials*, 2019, **6**, 022001.
15. Y. H. Lee, X. Q. Zhang, W. Zhang, M. T. Chang, C. T. Lin, K. D. Chang, Y. C. Yu, J. T. W. Wang, C. S. Chang and L. J. Li, *Advanced Materials*, 2012, **24**, 2320-2325.
16. K. Kang, S. Xie, L. Huang, Y. Han, P. Y. Huang, K. F. Mak, C.-J. Kim, D. Muller and J. Park, *Nature*, 2015, **520**, 656-660.
17. J. Chai, S. Tong, C. Li, C. Manzano, B. Li, Y. Liu, M. Lin, L. Wong, J. Cheng and J. Wu, *Advanced Materials*, 2020, **32**, 2002704.
18. Z. Cai, B. Liu, X. Zou and H.-M. Cheng, *Chemical Reviews*, 2018, **118**, 6091-6133.
19. Y.-F. Lim, K. Priyadarshi, F. Bussoletti, P. K. Gogoi, X. Cui, M. Yang, J. Pan, S. W. Tong, S. Wang and S. J. Pennycook, *ACS Nano*, 2018, **12**, 1339-1349.
20. Y. Liu, J. Guo, E. Zhu, L. Liao, S.-J. Lee, M. Ding, I. Shakir, V. Gambin, Y. Huang and X. Duan, *Nature*, 2018, **557**, 696-700.
21. Y. Wang, J. C. Kim, R. J. Wu, J. Martinez, X. Song, J. Yang, F. Zhao, A. Mkhoyan, H. Y. Jeong and M. Chhowalla, *Nature*, 2019, **568**, 70-74.
22. Y. Liu, P. Stradins and S.-H. Wei, *Science Advances*, 2016, **2**, e1600069.
23. A. Allain, J. Kang, K. Banerjee and A. Kis, *Nature Materials*, 2015, **14**, 1195-1205.
24. P.-C. Shen, C. Su, Y. Lin, A.-S. Chou, C.-C. Cheng, J.-H. Park, M.-H. Chiu, A.-Y. Lu, H.-L. Tang and M. M. Tavakoli, *Nature*, 2021, **593**, 211-217.
25. J. W. Chai, M. Yang, M. Callsen, J. Zhou, T. Yang, Z. Zhang, J. S. Pan, D. Z. Chi, Y. P. Feng and S. J. Wang, *Advanced Materials Interfaces*, 2017, **4**, 1700035.
26. B. Wang, W. Huang, L. Chi, M. Al-Hashimi, T. J. Marks and A. Facchetti, *Chemical Reviews*, 2018, **118**, 5690-5754.
27. W. Li, J. Zhou, S. Cai, Z. Yu, J. Zhang, N. Fang, T. Li, Y. Wu, T. Chen and X. Xie, *Nature Electronics*, 2019, **2**, 563-571.
28. Y. Y. Illarionov, T. Knobloch, M. Jech, M. Lanza, D. Akinwande, M. I. Vexler, T. Mueller, M. C. Lemme, G. Fiori and F. Schwierz, *Nature Communications*, 2020, **11**, 1-15.

29. X. Zou, J. Wang, C. H. Chiu, Y. Wu, X. Xiao, C. Jiang, W. W. Wu, L. Mai, T. Chen and J. Li, *Advanced Materials*, 2014, **26**, 6255-6261.
30. J. Robertson, *Reports on Progress in Physics*, 2005, **69**, 327.
31. D. Jena and A. Konar, *Physical Review Letters*, 2007, **98**, 136805.
32. G.-H. Lee, Y.-J. Yu, X. Cui, N. Petrone, C.-H. Lee, M. S. Choi, D.-Y. Lee, C. Lee, W. J. Yoo and K. Watanabe, *ACS Nano*, 2013, **7**, 7931-7936.
33. X. Cui, G.-H. Lee, Y. D. Kim, G. Arefe, P. Y. Huang, C.-H. Lee, D. A. Chenet, X. Zhang, L. Wang and F. Ye, *Nature Nanotechnology*, 2015, **10**, 534-540.
34. Y. Y. Illarionov, A. G. Banshchikov, D. K. Polyushkin, S. Wachter, T. Knobloch, M. Thesberg, L. Mennel, M. Paur, M. Stöger-Pollach and A. Steiger-Thirsfeld, *Nature Electronics*, 2019, **2**, 230-235.
35. S. McDonnell, B. Brennan, A. Azcatl, N. Lu, H. Dong, C. Buie, J. Kim, C. L. Hinkle, M. J. Kim and R. M. Wallace, *ACS Nano*, 2013, **7**, 10354-10361.
36. H. Liu and D. Y. Peide, *IEEE Electron Device Letters*, 2012, **33**, 546-548.
37. H. G. Kim and H.-B.-R. Lee, *Chemistry of Materials*, 2017, **29**, 3809-3826.
38. J. Tao, J. Chai, Z. Zhang, J. Pan and S. Wang, *Applied Physics Letters*, 2014, **104**, 232110.
39. P. Xia, X. Feng, R. J. Ng, S. Wang, D. Chi, C. Li, Z. He, X. Liu and K.-W. Ang, *Scientific Reports*, 2017, **7**, 1-9.
40. Y. Pan, K. Jia, K. Huang, Z. Wu, G. Bai, J. Yu, Z. Zhang, Q. Zhang and H. Yin, *Nanotechnology*, 2019, **30**, 095202.
41. Y. Hu, P. San Yip, C. W. Tang, K. M. Lau and Q. Li, *Semiconductor Science and Technology*, 2018, **33**, 045005.
42. J. H. Park, S. Fathipour, I. Kwak, K. Sardashti, C. F. Ahles, S. F. Wolf, M. Edmonds, S. Vishwanath, H. G. Xing and S. K. Fullerton-Shirey, *ACS nano*, 2016, **10**, 6888-6896.
43. G. Kresse and J. Hafner, *Physical Review B*, 1993, **47**, 558.
44. J. P. Perdew, K. Burke and M. Ernzerhof, *Physical Review Letters*, 1996, **77**, 3865.
45. P. E. Blöchl, *Physical Review B*, 1994, **50**, 17953.
46. X. Wu, M. Vargas, S. Nayak, V. Lotrich and G. Scoles, *The Journal of Chemical Physics*, 2001, **115**, 8748-8757.
47. M. Yang, J. W. Chai, M. Callsen, J. Zhou, T. Yang, T. T. Song, J. S. Pan, D. Z. Chi, Y. P. Feng and S. J. Wang, *The Journal of Physical Chemistry C*, 2016, **120**, 9804-9810.
48. M. Yang, C. Zhang, S. Wang, Y. Feng and Ariando, *AIP Advances*, 2011, **1**, 032111.
49. X.-s. Wang, G. Zhai, J. Yang and N. Cue, *Physical Review B*, 1999, **60**, R2146.
50. M. Yang, R. Wu, W. Deng, L. Shen, Z. Sha, Y. Cai, Y. Feng and S. Wang, *Journal of Applied Physics*, 2009, **105**, 024108.
51. V. Bermudez, *Surface Science*, 2005, **579**, 11-20.
52. L. Bengtsson, *Physical Review B*, 1999, **59**, 12301.
53. T. Ma, *IEEE Transactions on Electron Devices*, 1998, **45**, 680-690.
54. W. Zhu, D. Neumayer, V. Perebeinos and P. Avouris, *Nano Letters*, 2010, **10**, 3572-3576.
55. M. Yang, J. Chai, Y. Wang, S. Wang and Y. Feng, *The Journal of Physical Chemistry C*, 2012, **116**, 22315-22318.
56. B. Huang, Q. Xu and S.-H. Wei, *Physical Review B*, 2011, **84**, 155406.
57. W. Scopel, R. Miwa, T. Schmidt and P. Venezuela, *Journal of Applied Physics*, 2015, **117**, 194303.
58. Y.-J. Kang, J. Kang and K.-J. Chang, *Physical Review B*, 2008, **78**, 115404.
59. K. Kamiya, N. Umezawa and S. Okada, *Physical Review B*, 2011, **83**, 153413.
60. K. Dolui, I. Rungger and S. Sanvito, *Physical Review B*, 2013, **87**, 165402.
61. J. Martin, N. Akerman, G. Ulbricht, T. Lohmann, J. v. Smet, K. Von Klitzing and A. Yacoby, *Nature Physics*, 2008, **4**, 144-148.
62. S. Ashok, *Research in Hydrogen Passivation of Defects and Impurities in Silicon: Final Report, 2 May 2000-2 July 2003*, National Renewable Energy Lab., Golden, CO (US), 2004.

63. T. Yang, Y. Bao, W. Xiao, J. Zhou, J. Ding, Y. P. Feng, K. P. Loh, M. Yang and S. J. Wang, *ACS Applied Materials & Interfaces*, 2018, **10**, 22042-22049.
64. S. M. Sze, *Semiconductor devices: physics and technology*, John Wiley & Sons, 2008.
65. H. Liu, K. Xu, X. Zhang and P. D. Ye, *Applied Physics Letters*, 2012, **100**, 152115.
66. D. M. Hausmann, E. Kim, J. Becker and R. G. Gordon, *Chemistry of Materials*, 2002, **14**, 4350-4358.
67. M. Yang, A. Nurbawono, C. Zhang, Y. P. Feng and Ariando, *Applied Physics Letters*, 2010, **96**, 193115.
68. M. Z. Rahman, C. W. Kwong, K. Davey and S. Z. Qiao, *Energy & Environmental Science*, 2016, **9**, 709-728.